OUTAGE PERFORMANCE EVALUATION OF DEVICE-TO-DEVICE SYSTEM WITH ENERGY HARVESTING RELAY

Miloš SIMONOVIĆ*, *Aleksandra CVETKOVIĆ, Jelena MANOJLOVIĆ, Vlastimir NIKOLIĆ*

University of Nis, Faculty of Mechanical Engineering, Nis, Serbia

* Corresponding author; E-mail: milos.simonovic@masfak.ni.ac.rs

The development of Internet of Things (IoT) devices as well as the increase of nodes in wireless networks, motivates the use of node's cooperation for wireless system performance improvement. On the other hand, the power requirements of the increasing number of nodes leads to the need for new powering sources. In this paper we consider device-to-device (D2D) relay-assisted system, where decode-and-forward (DF) relay is not equipped with its own power supply, but it harvests energy and uses it for the data transfer to the destination node. System performance is derived for the Fisher-Snedecor F composite fading channel model and energy harvesting protocol based on time-switching scheme. The closed-form approximate expression for the outage probability is derived, that corresponds to the exact results. The impact of the channel fading and shadowing parameters and time-switching factor of energy harvesting protocol on the system performances are investigated. Numerical results are confirmed by an independent simulation method.

Key words*: Decode-and-forward (DF) relay, Device-to-device (D2D) communication, Energy harvesting (EH), Outage probability, Time-switching relaying (TSR) protocol*

1. Introduction

The development of Internet of Things (IoT) accelerated the increase of the number of connected devices and additionally contributed to the significance of wireless sensor networks (WSN). IoT technology has broad range of applications in industry, agriculture, traffic, ...[1-2]. IoT and WSN are used with an aim to increase the efficiency and overall quality of life (smart home, smart grid, smart city,...) [3-4]. Industrial Internet of Things (IIoT) is closely related to the fourth industrial revolution, Industria 4.0. Measurements and optimization of industrial processes in IIOT systems are provided using various sensors, so the need for processing of big data quantity arises [5-6]. Wireless body sensor networks (WBSN) are especially important as they enable communication among sensors located on human's body and remote diffusion centers for gathering and processing of data [7-8].

Apart from the expected increase of total traffic, the raised number of users leads also to the increased energy usage that may cause potential ecological issues. Therefore, the way to increase energy efficiency is highly required [9]. The sensors and devices are with limited battery power, that need replacement or additional charging. The demand for the battery replacement is considered to be one of the drawbacks of the WSN, as nodes can be positioned in remote and inaccessible areas. In

order to prolong the device lifetime, the energy harvesting (EH) technologies from various sources can be used (solar energy, mechanical vibration, thermal energy, wind, ...) [10,11]. The devices can combine the capabilities of the wireless communications and energy harvesting in order to provide data transfer without the explicit need for the external sources [9, 12].

Cooperative techniques are widely used for the increase of coverage area, improvement of signal transmission reliability and quality of service in WSN. Data transfer from each node to the sink node or gateway node is provided by cooperation among sensors. In the case when direct communication between source and destination node is not possible, it is enabled by using the devices that have the relay function. Based on the type of relay node, they can be classified as amplify-and-forward (AF) and decode-and-forward (DF) relays. AF relay amplifies the signal by constant or variable gain, depending on the channel state information (CSI), while complete regeneration is performed in the case of DF relays [13]. The application of EH technology is especially important in cooperative wireless networks, where high reliability and spectral efficiency that cooperative transmission provides can be united with flexible and efficient device powering solutions [12].

Cooperative relay network with EH harvesting from RF sources is analyzed in [14]. The energy and data transfer is based on the TSR (time-switching relaying) and PSR (power-splitting relaying) protocols. In the first approach total time frame is divided in two non-overlapping intervals dedicated to the energy and data transfer, while in the second one total harvested energy is split into parts dedicated for the energy accumulation and data transfer. As the wireless link is used for the data transfer in wireless networks, system performances depend on the channel characteristics, so fading and shadowing effects should be carefully considered. In wireless channels fading can be modelled using various distributions, such as Rayleigh, Nakagami, Rice,… Although it is well known that shadowing effect is usually modelled by lognormal distribution, the Gama distribution is also often used as it enables more elegant mathematical derivations and provides clear insight into system performances on the basis of derived analytical results [15]. Generalized-K composite fading encompasses both fading and shadowing effects and it was used for a long time as the most general and comprehensive channel model. Futhermore, the Fisher-Snedecor F fading model was proposed recently [16]. Its main advantages are excellent agreement with the experimentally collected data and probability density function (PDF) expression consists only of elementary functions [16-17]. The communication system over Fisher-Snedecor F comosite fading can be applyed for healthcare and fitness purposes due to fact that this composite fading shows accurate fit to experimental measurements for WBSN. Exact and asymptotic ergodic capacity expressions over Fisher-Snedecor F fading channels using power adaption methods are presented in [17] while in [18] performances of multiple branch maximal-ratio combining (MRC) system are investigated. Performance of D2D system over Fisher-Snedecor F channel in the presence of co-channel interference can be found in [19].

In this paper we consider D2D communication with DF relay-assisted system. The network with relay nodes increases coverage area and improves achievable throughput for the case when the devices are too far away from each other or when the direct D2D communication is disabled. We assume that the relay does not have an external power source and it collects radio frequency (RF) energy from the transmitter for power supply. The performance of cooperative systems with EH relay over channels where only the impact of fading is considered can be found in open literature. For example, DF relaying system with TSR and PSR energy harvesting protocol in Rayleigh fading environment is

analysed in [20] while in [21] throughout performances of AF and DF relay-assisted communication system over Nakagami-*m* fading channel are derived. Energy harvesting applications in scenarios with both fading and shadowing effects are presented in [22-23]. To the best authors' knowledge, analysis of D2D communication with EH DF relay-assisted network over Fisher-Snedecor F model is not available in the literature. We derived novel approximate closed-form expressions of outage probability for the case when energy harvesting and information transmission is performed based on TSR protocol. Numerical results are obtained based on the derived analytical expressions and obtain results allow analysis of the influence of channel and EH parameters on the outage performance. Analytical results for outage probability and outage capacity are validated via independent simulation method.

2. System and channel model

The considered system consists of devices (D_1 and D_2) which communicate via DF relay node R as shown in the Fig. 1. The direct link between devices is disabled (due to large distance or low channel quality between the devices for direct communication) and they communicate only via relay node R. The signal transmission is performed over the wireless links in which the influence of fading and the shadowing effect cannot be neglected. Composite Fisher-Snedecor F channel model can be applied for both line-of-sight (LoS) and non-LoS (NLoS) environments and can efficiently model various conditions of fading and shadowing [19, 24]. This fading model includes some special cases such as the Nakagami-*m* distribution, Rayleigh distribution, and one-sided Gaussian distribution.
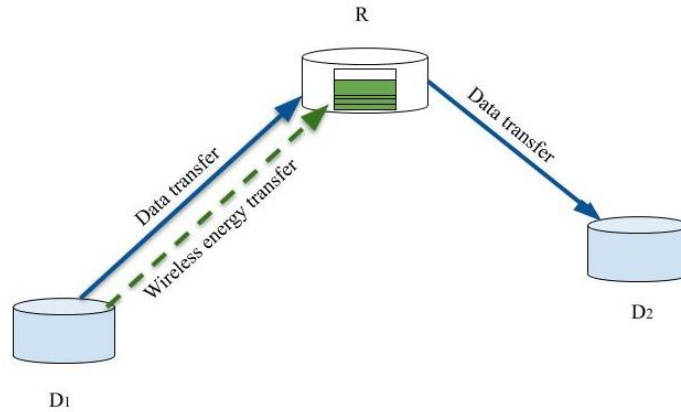
Figure 1. System model of cooperative relaying system where the relay harvests RF energy from the source

In Fisher-Snedecor F composite channel, multipath fading is modelled by Nakagami-*m* distribution and the variation of root mean square power is subject to inverse Nakagami-*m* distribution. The PDF of channel power gains for D_1-R link node, γ_1, and relay-device D_2 link, γ_2, over Fisher-Snedecor F distributed channel have the form [16]

$$p_{\gamma_i}(x) = \frac{m_i^{m_i}(m_{si}\bar{\gamma}_i)^{m_{si}}}{B(m_i, m_{si})} \frac{x^{m_i-1}}{(m_i x + m_{si}\bar{\gamma}_i)^{m_i+m_{si}}} = \frac{\left(\dfrac{m_i}{m_{si}\bar{\gamma}_i}\right)^{m_i}}{B(m_i, m_{si})} \frac{x^{m_i-1}}{\left(\dfrac{m_i x}{m_{si}\bar{\gamma}_i}+1\right)^{m_i+m_{si}}}, \tag{1}$$

where B(·,·) denotes Beta function [25, eq. (8.31)], $\bar{\gamma}_i = E[\gamma_i]$ is average SNR over i-th channel, while m_{mi} and m_{si} denote the multipath fading and shadowing parameters, respectively. The cumulative density function (CDF) can be obtained in the form of hypergeometric function [16] or in the following form

$$F_{\gamma_i}\left(\gamma_{th}\right)=\left(\frac{m_i\gamma_{th}}{m_{si}\bar{\gamma}_i}\right)^{m_i}\frac{1}{\Gamma\left(m_i+m_{si}\right)B\left(m_i,m_{si}\right)}G_{2,2}^{1,2}\left(\frac{m_i\gamma_{th}}{m_{si}\bar{\gamma}_1}\left|\begin{matrix}1-m_i,1-m_i-m_{si}\\0,-m_i\end{matrix}\right.\right),\tag{2}$$

where $\Gamma(\cdot)$ denotes Gamma function [25, eq. (8.31)] and $G_{p,q}^{m,n}(\cdot)$ denotes Meijer's G-function [25, eq. (9.301)]. Special functions (Meijer's G-function, Gamma and Beta function) are built in Wolfram Mathematica software package.

In the D2D system under study, the communication between devices is enabled with assistance of relay. Assuming that the relay has constrain battery power, alternative power supplies are required, thus it harvests RF energy from the source as shown in the Fig.1. TSR protocol is performed in which energy harvesting and data transmission are applied within the frame duration T as illustrated in Fig. 2. During the frame duration the channel coefficient is constant but it changes independently from frame to frame. Within a frame, the part of the frame duration, αT (0<α<1) is used to supply the power to the relay and the rest of the frame duration is used for data transmission. The transmission time (1-α)T is divided into equal intervals, thus (1-α)T/2 is the time for signal transmission from device to relay and the other (1-α)T/2 interval time is reserved for relay-device transmission [14]. The time frame allocation of the TSR protocol is shown in the Fig. 2.

D_1 Energy transfer → R	D_1 Data transfer → R	R Data transfer → D_2
αT	(1-α)T/2	(1-α)T/2
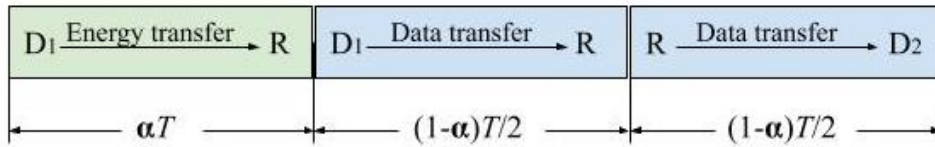
Figure 2. TSR protocol for energy harvesting and data transfer

The source D_1 transmits the signal s with the power P_S. The channel fading gain between the D_1 and the R is h_1, the received signal at the relay node is given by

$$y_R = \sqrt{P_S}h_1 s + n_1,\tag{3}$$

where n_1 is the additive white Gaussian noise (AWGN) component at the relay node with the power σ_1^2. During the frame interval αT, the relay supplies energy from the source device and overall harvested energy at each frame is

$$E_H = \eta P_S \gamma_1 \alpha T,\tag{4}$$

where η (0<η<1) denotes the energy conversion efficiency and channel power gain for D_1-R is $\gamma_1 = |h_1|^2$.

We assume that all harvested energy from the received signal is consumed for relay data transmission to the destination device. Therefore, from (4), the relay transmitted power P_R is given by

$$P_R = \frac{E_H}{\left(1-\alpha\right)T/2} = \frac{2\eta\alpha}{\left(1-\alpha\right)}P_S\gamma_1.\tag{5}$$

The received signal at the destination is

$$y_D = \sqrt{P_R} h_2 s_R + n_2,$$ (6)

where s_R is the decoded information signal sent from the relay, and n_2 is the AWGN component at the destination with the variance σ_2^2.

The received signal-to-noise ratio (SNR) at the relay node using (3) is defined as

$$\gamma_R = \frac{P_S}{\sigma_1^2} \gamma_1.$$ (7)

while SNR at the destination device based on (5) and (6) can be expressed as

$$\gamma_D = \frac{2\eta\alpha}{(1-\alpha)\sigma_2^2} P_S \gamma_1 \gamma_2.$$ (8)

By introducing constants $c_1 = P_S / \sigma_1^2$ and $c_2 = 2\eta\alpha\sigma_1^2 / \left((1-\alpha)\sigma_2^2\right)$, the SNR at the relay and the destination device can be written as $\gamma_R = c_1 \gamma_1$ and $\gamma_D = c_1 c_2 \gamma_1 \gamma_2$, respectively.

For the considered cooperative D2D system with energy harvesting relay, we analyse the outage probability and outage capacity, as important performance metrics.

3. Outage analysis

Due to the fading and the shadowing effects, the wireless channel is time-varying so the received signal power at the devices is not constant. The consequence is that the current SNR can be described as a random variable. Therefore, the outage probability is a measure which represents the probability that a quality of service is not supported due to variable SNR. Further, the largest data rate that can be achieved in the time-variation channel with the specified outage probability, represents the outage capacity.

For DF relaying system, the outage probability is defined as the probability that the received SNR at the relay node or destination node is below the predetermined threshold, γ_{th}. Therefore, it can be calculated as

$$P_{out} = \Pr\{\gamma_R \le \gamma_{th}\} + \Pr\{\gamma_D \le \gamma_{th}, \gamma_R > \gamma_{th}\}.$$ (9)

Using $\gamma_R = c_1 \gamma_1$ and $\gamma_D = c_1 c_2 \gamma_1 \gamma_2$, (9) becomes

$$P_{out} = F_{\gamma_1}\left(\frac{\gamma_{th}}{c_1}\right) + \int_{\gamma_{th}}^{\infty} F_{\gamma_2}\left(\frac{\gamma_{th}}{c_2 \gamma_1}\right) p_{\gamma_1}(\gamma_1) \mathrm{d}\gamma_1,$$ (10)

where $F_{\gamma_1}(x)$ and $F_{\gamma_2}(x)$ are given by (2) for i=1, 2, respectively. The probability in integral form which exists in (10) cannot be solved in the exact closed-form. In order determined the expression for outage probability, (10) can be rewritten as

$$P_{out} = F_{\gamma_1}\left(\frac{\gamma_{th}}{c_1}\right) + \int_{0}^{\infty} F_{\gamma_2}\left(\frac{\gamma_{th}}{c_2 \gamma_1}\right) p_{\gamma_1}(\gamma_R) \mathrm{d}\gamma_R - \int_{0}^{\gamma_{th}} F_{\gamma_2}\left(\frac{\gamma_{th}}{c_2 \gamma_1}\right) p_{\gamma_1}(\gamma_R) \mathrm{d}\gamma_R = F_{\gamma_1}\left(\frac{\gamma_{th}}{c_1}\right) + I_1 - I_2,$$ (11)

where I_1 and I_2 are defined as

$$I_1 = \int_{0}^{\infty} F_{\gamma_2}\left(\frac{\gamma_{th}}{c_2 \gamma_1}\right) p_{\gamma_1}(\gamma_1) \mathrm{d}\gamma_1,$$ (12)

$$I_2 = \int_0^{\gamma_{th}} F_{\gamma_2}\left(\frac{\gamma_{th}}{c_2\gamma_1}\right) p_{\gamma_1}(\gamma_1)d\gamma_1, \tag{13}$$

respectively.

Substituting (1) for $i=1$ and (2) for $i=2$ in (12), the integral has the form

$$I_1 = \frac{\left(\dfrac{c_1 m_{s1}\overline{\gamma}_1}{m_1}\right)^{-m_1}\left(\dfrac{m_2\gamma_{th}}{c_2 m_{s2}\overline{\gamma}_2}\right)^{m_2}}{\Gamma(m_2+m_{s2})B(m_1,m_{s1})B(m_2,m_{s2})}$$

$$\times \int_0^\infty \gamma_1^{m_1-1-m_2}\left(\frac{m_1\gamma_1}{c_1 m_{s1}\overline{\gamma}_1}+1\right)^{-m_1-m_{s1}} G_{2,2}^{1,2}\left(\frac{m_2\gamma_{th}}{m_{s2}\overline{\gamma}_2 c_2\gamma_1}\left|\begin{matrix}1-m_2,1-m_2-m_{s2}\\0,-m_2\end{matrix}\right.\right)d\gamma_1. \tag{14}$$

Using representation of Meijer's G-function in terms *of* polynomials [26, 01.02.26.0007.01] as

$$\left(\frac{m_1\gamma_1}{c_1 m_{s1}\overline{\gamma}_1}+1\right)^{-m_1-m_{s1}} = \frac{1}{\Gamma(m_1+m_{s1})}G_{1,1}^{1,1}\left(\frac{m_1\gamma_1}{c_1 m_{s1}\overline{\gamma}_1}\left|\begin{matrix}1-m_1-m_{s1}\\0\end{matrix}\right.\right), \tag{15}$$

we get

$$I_1 = \frac{\left(\dfrac{c_1 m_{s1}\overline{\gamma}_1}{m_1}\right)^{-m_1}\left(\dfrac{m_2\gamma_{th}}{c_2 m_{s2}\overline{\gamma}_2}\right)^{m_2}}{\Gamma(m_1+m_{s1})\Gamma(m_2+m_{s2})B(m_1,m_{s1})B(m_2,m_{s2})}$$

$$\int_0^\infty \gamma_1^{m_1-1-m_2}G_{1,1}^{1,1}\left(\frac{m_1\gamma_1}{c_1 m_{s1}\overline{\gamma}_1}\left|\begin{matrix}1-m_1-m_{s1}\\0\end{matrix}\right.\right)G_{2,2}^{1,2}\left(\frac{m_2\gamma_{th}}{m_{s2}\overline{\gamma}_2 c_2\gamma_1}\left|\begin{matrix}1-m_2,1-m_2-m_{s2}\\0,-m_2\end{matrix}\right.\right)d\gamma_1. \tag{16}$$

The closed-form solution for I_1 is determined applying [26, 07.34.16.0002.01] and further using [26, 07.34.21.0011.01] in the form

$$I_1 = \frac{\left(\dfrac{m_1 m_2\gamma_{th}}{c_1 c_2 m_{s1} m_{s2}\overline{\gamma}_2\overline{\gamma}_1}\right)^{m_2}}{\Gamma(m_1+m_{s1})\Gamma(m_2+m_{s2})B(m_1,m_{s1})B(m_2,m_{s2})}G_{3,3}^{3,2}\left(\frac{c_1 c_2 m_{s1} m_{s2}\overline{\gamma}_1\overline{\gamma}_2}{m_1 m_2\gamma_{th}}\left|\begin{matrix}1,1-m_1+m_2,1+m_2\\m_2,m_2+m_{s2},m_2+m_{s1}\end{matrix}\right.\right). \tag{17}$$

By applying the same transformations as with I_1, the probability given by integral I_2 can be rewritten as

$$I_2 = \frac{\left(\dfrac{c_1 m_{s1}\overline{\gamma}_1}{m_1}\right)^{-m_1}\left(\dfrac{m_2\gamma_{th}}{c_2 m_{s2}\overline{\gamma}_2}\right)^{m_2}}{\Gamma(m_1+m_{s1})\Gamma(m_2+m_{s2})B(m_1,m_{s1})B(m_2,m_{s2})}$$

$$\times \int_0^{\gamma_{th}} \gamma_1^{m_1-1-m_2}G_{1,1}^{1,1}\left(\frac{m_1\gamma_1}{c_1 m_{s1}\overline{\gamma}_1}\left|\begin{matrix}1-m_1-m_{s1}\\0\end{matrix}\right.\right)G_{2,2}^{2,1}\left(\frac{m_{s2}\overline{\gamma}_2 c_2\gamma_1}{m_2\gamma_{th}}\left|\begin{matrix}1,1+m_2\\m_2,m_2+m_{s2}\end{matrix}\right.\right)d\gamma_1. \tag{18}$$

The closed-form expression due to finite bound of integral cannot be obtain. For small values of the argument of first Meijer's G-function, using [26, 07.34.06.0001.01], the first Meijer's G-function can be approximated as

$$G_{1,1}^{1,1}\left(\frac{m_1\gamma_R}{c_1 m_{s1}\overline{\gamma}_1}\left|\begin{matrix}1-m_1-m_{s1}\\0\end{matrix}\right.\right) \approx \Gamma(m_1+m_{s1})\left(\frac{m_1\gamma_R}{c_1 m_{s1}\overline{\gamma}_1}\right)^0. \tag{19}$$

So, the (18) becomes

$$
I_2 \approx \frac{\left(\dfrac{c_1 m_{s1}\bar{\gamma}_1}{m_1}\right)^{-m_1}\left(\dfrac{m_2\gamma_{th}}{c_2 m_{s2}\bar{\gamma}_2}\right)^{m_2}}{\Gamma(m_2+m_{s2})B(m_1,m_{s1})B(m_2,m_{s2})}\int_0^{\gamma_{th}}\gamma_1^{m_1-1-m_2}G_{2,2}^{2,1}\left(\frac{m_{s2}\bar{\gamma}_2 c_2 \gamma_1}{m_2\gamma_{th}}\left|\begin{matrix}1,1+m_2\\ m_2,m_2+m_{s2}\end{matrix}\right.\right)d\gamma_1. \tag{20}
$$

The approximate expression for the integral I_2 in the exact closed-form is derived based on [26, 07.34.21.0084.01]

$$
I_2 \approx \frac{\left(\dfrac{m_1\gamma_{th}}{c_1 m_{s1}\bar{\gamma}_1}\right)^{m_1}\left(\dfrac{m_2}{c_2 m_{s2}\bar{\gamma}_2}\right)^{m_2}}{\Gamma(m_2+m_{s2})B(m_1,m_{s1})B(m_2,m_{s2})}G_{3,3}^{2,2}\left(\frac{m_{s2}\bar{\gamma}_2 c_2}{m_2}\left|\begin{matrix}1-m_1+m_2,1,1+m_2\\ m_2,m_2+m_{s2},m_2-m_1\end{matrix}\right.\right). \tag{21}
$$

Finally, the closed-form analytic expression for outage probability is obtained by substituting (17) and (21) into (11) as

$$
\begin{aligned}
P_{out} &\approx \left(\frac{m_1\gamma_{th}}{c_1 m_{s1}\bar{\gamma}_1}\right)^{m_1}\frac{1}{\Gamma(m_1+m_{s1})B(m_1,m_{s1})}G_{2,2}^{1,2}\left(\frac{m_1\gamma_{th}}{c_1 m_{s1}\bar{\gamma}_1}\left|\begin{matrix}1-m_1,1-m_1-m_1\\ 0,-m_1\end{matrix}\right.\right)\\
&+\frac{\left(\dfrac{m_1 m_2\gamma_{th}}{c_1 c_2 m_{s1}m_{s2}\bar{\gamma}_2\bar{\gamma}_1}\right)^{m_2}}{\Gamma(m_1+m_{s1})\Gamma(m_2+m_{s2})B(m_1,m_{s1})B(m_2,m_{s2})}G_{3,3}^{3,2}\left(\frac{c_1 c_2 m_{s1}m_{s2}\bar{\gamma}_1\bar{\gamma}_2}{m_1 m_2\gamma_{th}}\left|\begin{matrix}1,1-m_1+m_2,1+m_2\\ m_2,m_2+m_{s2},m_2+m_{s1}\end{matrix}\right.\right)\\
&-\frac{\left(\dfrac{m_1\gamma_{th}}{c_1 m_{s1}\bar{\gamma}_1}\right)^{m_1}\left(\dfrac{m_2}{c_2 m_{s2}\bar{\gamma}_2}\right)^{m_2}}{\Gamma(m_2+m_{s2})B(m_1,m_{s1})B(m_2,m_{s2})}G_{3,3}^{2,2}\left(\frac{m_{s2}\bar{\gamma}_2 c_2}{m_2}\left|\begin{matrix}1-m_1+m_2,1,1+m_2\\ m_2,m_2+m_{s2},m_2-m_1\end{matrix}\right.\right).
\end{aligned} \tag{22}
$$

Later, it will be presented that the results obtained from the derived approximate expressions coincide perfectly with the simulation results which supports the accuracy of the approximate derived expression.

For determination the maximum data rate that can be achieved in the slowly varying channels, where instantaneous SNR is constant for a large number of symbols, the outage capacity measurement is used. The normalized capacity $\ln(1+\gamma_{th})$ with a probability $(1-P_{out})$ leads to outage capacity expression [27]

$$
C_{out} = \frac{1}{2\ln 2}\left(1-P_{out}(\gamma_{th})\right)\ln(1+\gamma_{th}), \tag{23}
$$

Considering TSR protocol achievable throughput is determined by

$$
T_{out} = (1-\alpha)C_{out}. \tag{24}
$$

4. Numerical results

The influence of channel parameters and time-switching factor on outage performance is examined through numerical and simulation results. Numerical results are obtain using derived approximate closed-form eq. (22) and by numerical integration in eq. (11) to get exact results. Furthermore, the simulation results are obtained using independent Monte-Carlo simulation method. The outage probability and outage capacity values of simulation are estimated by averaging over 10^6

generated channel samples. The numerical and simulation results on Figs. 2 to 6 are obtained using the energy conversion efficiency η=0.8 and the noise power $\sigma_R^2 = \sigma_D^2 = 0.01$. The average channel gains set to one, $\bar{\gamma}_1 = \bar{\gamma}_2 = 1$. By specifying these parameters, the derived expressions and the presented analysis do not lose generality.

Outage probability in the function of time-switching factor for different values of transmit power P_S and for various propagation scenarios is presented in Fig. 3. As expected, with increasing transmit power the outage probability decreases. For a given specified outage probability value, the required time-switching factor has a higher value for the case of worse channel conditions. The better outage performance is observed for the higher values of the shadowing parameter which corresponds to the smaller shadowing effects. It is assumed that m_s=5 represents the moderate shadowing, m_s= 0.5 heavy shadowing and m_s= 50 corresponds to the light shadowing condition [18]. From the Fig.3. it can be noticed the accuracy of the approximate closed-form results (eq. 22) compared to exact results (eq. 11).
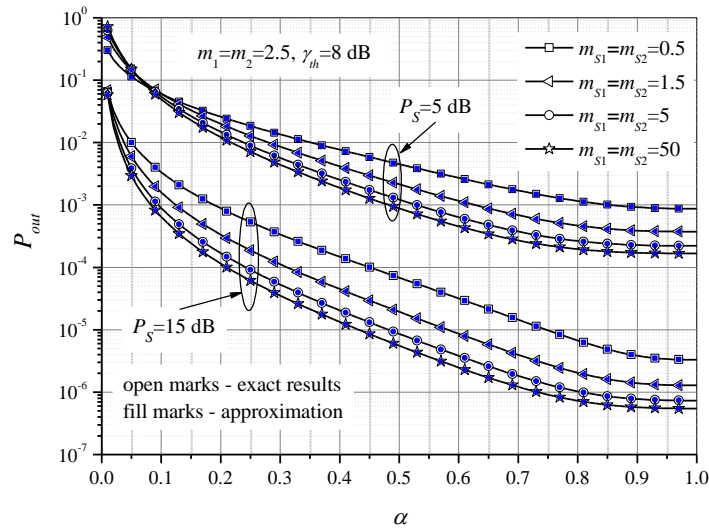

Figure 3. Outage probability versus time-switching factor, α, for various values of transmit power and shadowing conditions

In the Fig. 4. the outage probability versus transmit power for various channel parameter values is presented. The channel conditions of D_1-R and R-D_2 are different. The communication is analysed for the case when D_1-R link is exposed to heavy shadowing effect, while light shadowing is present over R-D_1 link and vice versa. The outage probability decreases when transmit power and time-switching factor increase. For the case of low value of α (α=0.2 and α =0.4) the difference in outage probability performances for the shadowing propagation scenarios (m_{s1}=0.5, m_{s2}=50) and (m_{s1}=50, m_{s2}=5) diminishes. This can be explained by the fact that the time for energy harvesting is short and therefore the transmit power of relay over R-D_2 link is too small. The performance of the system with DF relay is determined by link with smaller SNR, in this case R-D_2 (regardless of the channel shadowing effects). When time for energy harvesting is longer, SNR of R-D_2 (γ_R) link increases and SNR of R-D_1 (γ_D) becomes smaller then SNR of R-D_2 ($\gamma_R > \gamma_D$), so the influence of the shadowing effects of D_1-R link is reflected on the system performance. Smaller shadowing effect of D_1-R link leads to decrease of outage probability.
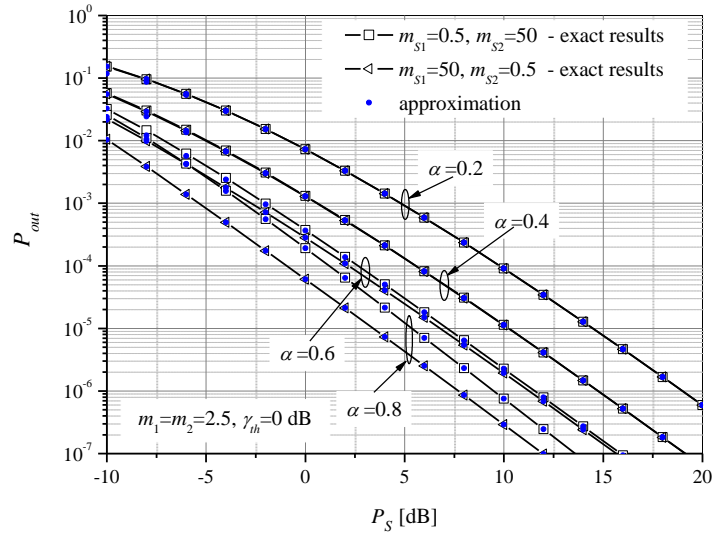
**Figure 4.** Outage probability versus transmit power for various values of α and shadowing parameters
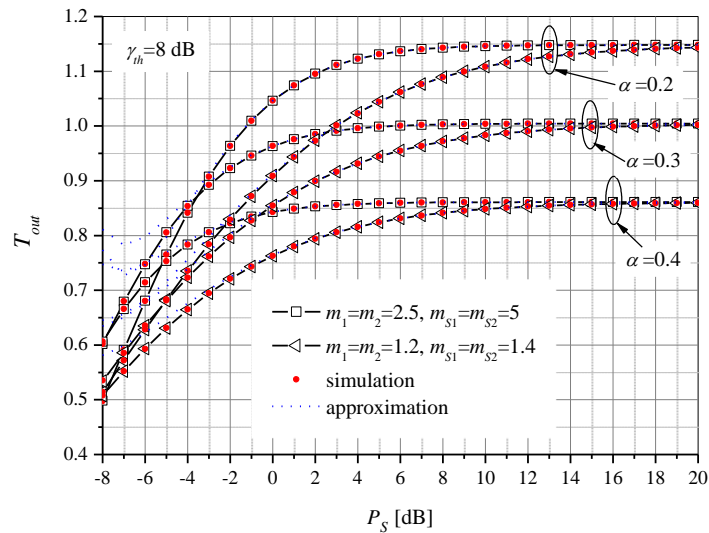
Figure 5. Throughput T_{out} versus transmit power

The dependence of achievable throughput on the power *Ps* is presented in Fig. 5. Numerical and simulation results are obtained for different values of time-switching factor and propagation environment conditions. The numerical results demonstrate excellent agreement between analytical and simulation results. The gap between derived and simulation results occurs at low values of transmit power because the approximation in this range is not valid due to fact that argument of Meijer's G-function is not small. With the increase of transmit power, the achievable throughput increases, and the throughput floor appears for large values of P_S. The floor value depends on the energy harvesting time but it is independent on the propagation conditions for certain values of α. The raise of α leads to the higher relay transmit power but it also leads to the decrease of the time interval for information transmission which is crucial for reducing achievable throughput.

The throughput based on the outage capacity in the function of time-switching factor is presented in Fig. 6 when the fading and shadowing parameters are the same in both links. The effect of transmit power on achievable throughput can be also noticed. With increasing Ps the throughput also increases. The results show that there is an optimum relay charging time, α, leading to maximum through value. Achievable throughput values increase when the fading and shadowing effect is reduced. On the other side, an optimal value of α that maximizes throughput increases with the degradation of the channel conditions e.g. it then takes more time to harvest energy at the relay.
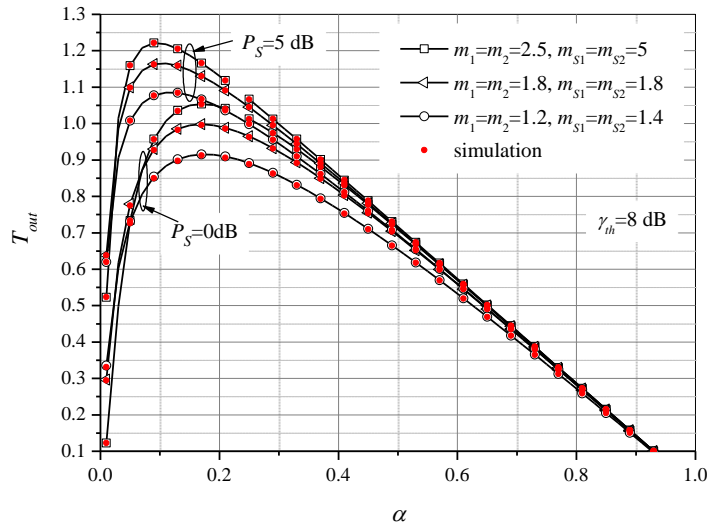
Figure 6. Throughput T_{out} versus time-switching factor α
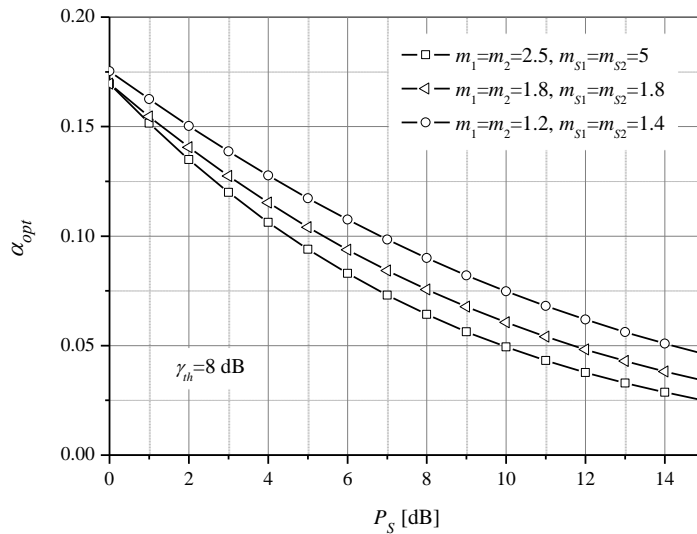
Figure 7. Optimal value of time-switching factor α in the function of transmit power

The optimal value of time-switching factor α that maximize throughput for certain environmental condition and system parameter can be determined. The optimal time-switching factor in the function of transmit power is calculated for channel condition parameters used in the Fig.6. and this dependence is presented in the Fig.7.

5. Conclusion

The outage performance of energy-constrained D2D relaying networks over Fisher-Snedecor F channels is analysed. Closed-form expressions for outage probability and outage capacity were obtained for the system with TSR scheme. Based on derived analytical expressions, numerical results were obtained and impact of fading and shadowing parameter on system performance was discussed. The influence of time-switching factor on outage probability and throughput was also examined. The optimal values of energy harvesting time-switching factor which maximizes achievable throughput is higher for the case of lower transmit power and the environment of dominant fading and shadowing effects. The accuracy of derived analytical results is confirmed by independent simulations results. The obtained results can be used for design of WBANs in order to determine the optimal values of the system parameters for an acceptable outage performance.

References

[1] Osamy, W., Khedr, A. M., Salim, A., ADSDA: Adaptive Distributed Service Discovery Algorithm for Internet of Things Based Mobile Wireless Sensor Networks, *IEEE Sensors Journal*, *19* (2019), 22, pp. 10869 – 10880, DOI: 10.1109/JSEN.2019.2930589

[2] Alvarez Gil, R. P., Johanyák, Z. C., and Kovács, T., Surrogate Model based Optimization of Traffic Lights Cycles and Green Period Ratios using Microscopic Simulation and Fuzzy Rule Interpolation, *International Journal of Artificial Intelligence*, *16* (2018), 1, pp. 20-40.

[3] Ghayvat, H.,. *et al*., WSN- and IOT-Based Smart Homes and Their Extension to Smart Buildings, *Sensors* , *15* (2015), 5, pp. 10350-10379, DOI No. 10.3390/s150510350

[4] Pirbhulal, S. *et al*., A Novel Secure IoT-Based Smart Home Automation System Using a Wireless Sensor Network, *Sensors*, *17* (2017), 1, pp. 1-19, DOI No. 10.3390/s17010069

[5] Kim D.-S., Tran-Dang H., *Industrial Sensors and Controls in Communication Networks: From Wired Technologies to Cloud Computing and the Internet of Things*, Springer, Switzerland, 2019.

[6] Xu, L. D., He, W., Li, S., Internet of Things in Industries: A Survey, I*EEE Transactions on Industrial Informatics*, *10* (2014), 4, pp. 2233 – 2243, DOI No. 10.1109/TII.2014.2300753

[7] Boulis, A., *et al*., Challenges in Body Area Networks for Healthcare, *IEEE Communication Magazine,* 50 (2012), pp. 100-106, DOI No. 10.1109/MCOM.2012.6194389

[8] Albu, A., Precup, R.-E., Teban, T.-A., Results and Challenges of Artificial Neural Networks Used for Decision-Making and Control in Medical Applications, *Facta Universitatis, Series: Mechanical Engineering*, *17* (2019), 3, pp. 285 – 308.

[9] Kamalinejad, P., *et al*., Wireless Energy Harvesting for the Internet of things, *IEEE Communications Magazine*, *53* (2015), 6, pp.102-108, DOI No. 10.1109/MCOM.2015.7120024

[10] Dragović, Nj., et al., Potential and Prospects for Implementation of Renewable Energy Sources in Serbia, *Thermal Science*, 23 (2019), 5B, pp. 2895-2907.

[11] Mentis, D., Electrifying Greece with Solar and Wind Energy, *Thermal Science*, 18 (2014), 3, pp. 709-720.

[12]   Ramezani, P., Jamalipour, A., Toward the Evolution of Wireless Powered Communication Networks for the Future Internet of Things, *IEEE Network*, *31* (2017), 6, pp. 62-69, DOI No. 10.1109/MNET.2017.1700006.

[13]   Dohler, M., Li, Y., *Cooperative Communications: Hardware, Channel and PHY*, John Wiley & Sons, Chichester, West Sussex, United Kingdom, 2010.

[14]   Nasir, A. A *et al*., Throughput and ergodic capacity of wireless energy harvesting based DF relaying network, *Proceedings,* IEEE International Conference on Communications (ICC), Sydney, Australia, 2014., pp. 4066-4071

[15]   Bithas, P.S., *et al*., On the performance analysis of digital communications over generalized-K fading channels, *IEEE Communications Letters*, *10* (2006), 5, pp. 353 - 355, DOI No. 10.1109/LCOMM.2006.1633320

[16]   Yoo, S. K., *et al*., The Fisher-Snedecor F distribution: A simple and accurate composite fading model, *IEEE Communications Letters*, *21* (2017), 7, pp. 1661-1664, DOI No. 10.1109/LCOMM.2017.2687438

[17]   Zhao, H., *et al*., Ergodic Capacity Under Power Adaption Over Fisher–Snedecor F Fading Channels, *IEEE Communications Letters*, *23* (2019), 3, pp. 546 - 549, DOI No. 10.1109/LCOMM.2019.2894648

[18]   Badarneh, O. S., On the Sum of Fisher-Snedecor F Variates and its Application to Maximal-Ratio Combining, *IEEE Wireless Communications Letters*, 7 (2018), 6, pp. 966 - 969, DOI No. 10.1109/LWC.2018.2836453

[19]   Hussain, Z., Mehdi, H., Performance Analysis of D2D Communication System over Fisher-Snedecor F Channels, *International Journal of Computer Science and Network Security*, *19* (2019), 3, pp. 138-146

[20]   Nasir, A. A., *et al*., Throughput and ergodic capacity of wireless energy harvesting based DF relaying network, *Proceedings,* IEEE International Conference on Communications 2014 (ICC), Sydney, Australia, 2014, pp. 4066-4071.

[21]   Chen, Y., Energy Harvesting for Wireless Relaying Systems, in: *Wireless Information and Power Transfer: A New Paradigm for Green Communications*, Springer, 2018, pp. 123-155.

[22]   Rabie, K. M., Adebisi, B., Alouini, M. S., Wireless Power Transfer in Cooperative DF Relaying Networks with Log-Normal Fading, *Proceedings,* IEEE Global Communications Conference 2016 (GLOBECOM), Washington, USA, 2016, pp. 1-6.

[23]   Blagojevic, V., Cvetkovic, A., Ivanis, P., Performance analysis of energy harvesting DF relay system in generalized-K fading environment, *Physical Communications*, vol. 28 (2018), pp. 190-200, DOI No. 10.1016/j.phycom.2018.04.006

[24]   Almehmadi, F. S., Badarneh, O. S., On the effective capacity of Fisher–Snedecor F fading channels, *Electronics Letters*, *54* (2018), 18, pp. 1068-1070, DOI No. 10.1049/el.2018.5479

[25]   Gradshteyn, I. S., Ryzhik, I. M., *Table of Integrals, Series, and Products*, Academic Press, London, UK, 2007.

[26]   Wolfram Research, Accessed on 28 December 2017, http://functions.wolfram.com

[27]   Gu, Y., Aïssa, S., RF-Based Energy Harvesting in Decode-and-Forward Relaying Systems: Ergodic and Outage Capacities, *IEEE Transactions on Wireless Communications*, *14* (2015), 11, pp. 6425-6434, DOI No. 10.1109/TWC.2015.2453418.